Experiment IX: Angular Correlation of Gamma Rays

Curran D. Muhlberger
University of Maryland, College Park
(Dated: May 9, 2008)

Using a pair of scintillation detectors and a coincidence circuit, we measured the angular correlation functions for γ-rays emitted from sodium and cobalt nuclei. Theoretical arguments predict that successive γ-rays emitted from the same spinning nucleus should be distributed anisotropically, and this is indeed what we obseve. Photons emitted via pair annihilation in sodium must exhibit a δ-function distribution to conserve momentum, and our measurements indicate that coincidence rates are strongly peaked at $\theta = 180°$ with a dropoff consistent with the finite size of the detectors. Furthermore, our Legendre polynomial coefficients of $A_{22} = 0.0977 \pm 0.0099$ and $A_{44} = -0.0011 \pm 0.0125$ are consistent with their theoretical values for 4-2-0 quadrupole-quadrupole transitions in nickel after adjusting for finite detector size. We also compared our data with the results of Monte Carlo simulations and found them to be in agreement.

I. INTRODUCTION

When two γ-rays are emitted in succession from an atomic nucleus, their directions are often correlated due to the physics of the emission process. In particular, when an excited nuclear state decays to the ground state through one or more intermediate states, the spin of the nucleus affects the angular distribution of the photons emitted during each transition. The relative probability that a photon will be emitted at an angle θ with respect to a previously emitted photon is denoted $W(\theta)$ and depends both on the angular momenta of the states involved in the transitions and on the multipole order of the emitted radiation. Dr. D. R. Hamilton derived the theoretical forms of W for dipole and quadrupole radiation and computed the relevant coefficients for all possible angular momenta [1]. Here we experimentally verify these results for ^{60}Co.

Other nuclear processes, including electron-positron pair annihilation, can also produce correlated γ-rays. Sodium-22 in particular exhibits a simple angular distribution suitable for evaluating our detection apparatus. After undergoing β^+ decay (a 90% scenario), the resulting positron is captured by an electron, and the pair annihilates to produce a pair of 511 keV γ-rays as diagrammed in Figure 1. As the momentum of the positronium system must be conserved, the photons must be emitted in opposite directions. Therefore, the angular distribution function for ^{22}Na is given by

$$W(\theta) = \delta(\theta - \pi) \tag{1}$$

Once we have calibrated the detection apparatus and coincidence circuit using the ^{22}Na source, whose physics are well-understood, we can consider the more complicated case of cobalt-60. Through β^- emission, the cobalt nucleus decays into an excited state of nickel. This state then decays to the ground state though an intermediate state with a lifetime of 8×10^{-13} s, shown in Figure 2. The γ-rays emitted during these two transitions are thus effectively in coincidence. Assuming spin states of $J_1, J_2, J_3 = 4, 2, 0$ and quadrupole-quadrupole transitions [2], the angular correlation function for ^{60}Co is described by

$$W(\theta) = 1 + \frac{1}{8}\cos^2(\theta) + \frac{1}{24}\cos^4(\theta) \tag{2}$$

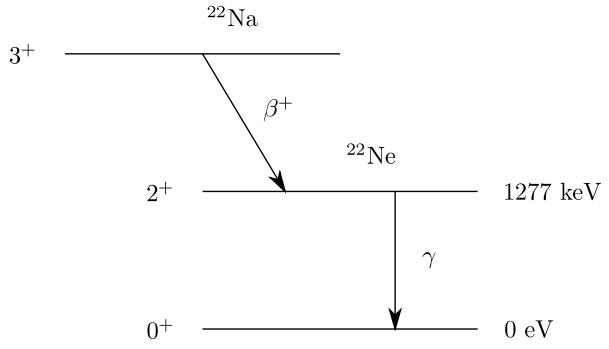

FIG. 1: Energy level diagram for the primary decay mechanism of sodium-22. The half-life of ^{22}Na is 2.6 yr and the initial β^+ decay occurs with 90% probability.

or equivalently

$$W(\theta) = 1 + A_{22}P_2(\cos(\theta)) + A_{44}P_4(\cos(\theta)) \tag{3}$$

where $A_{22} = 0.1020$, $A_{44} = 0.0091$, and P_n represent the Legendre polynomials. Note that $W(\theta)$ here gives the ratio of the likelihood of detecting a photon at an angle θ to the likelihood of detecting one at an angle of 90°. By experimentally measuring these angular correlation functions, we not only test the validity of the theory of correlated emission but also gain insight into the angular momenta of these decay processes.

We wish to detect not only the presence of γ-rays (with near-perfect efficiency), but also their energies. To do so we employ two NaI(Tl) scintillation detectors. When a high-energy γ-ray interacts with the sodium iodide crystal it produces a low-energy (visible) photon that is reflected towards an attached photomultiplier tube. Here it releases an electron from the cathode via the photoelectric effect, causing a cascade that is multiplied at each dynode in the tube to produce a voltage pulse at the anode whose height is proportional to the energy of the initial γ-ray.

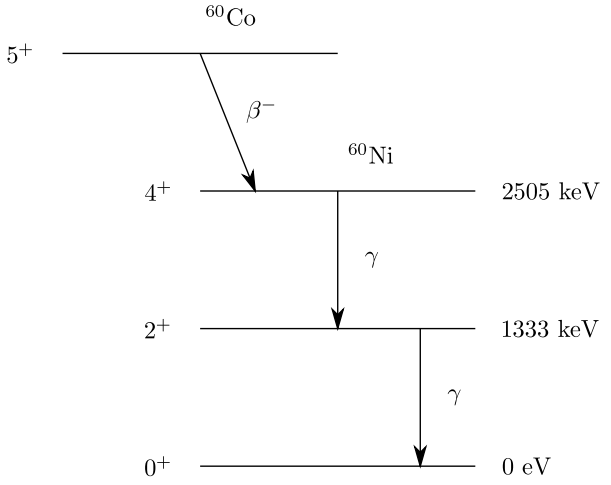

FIG. 2: Energy level diagram for the decay of cobalt-60. Half-life is 5.2 yr, and the intermediate state lives for 8×10^{-13} s.

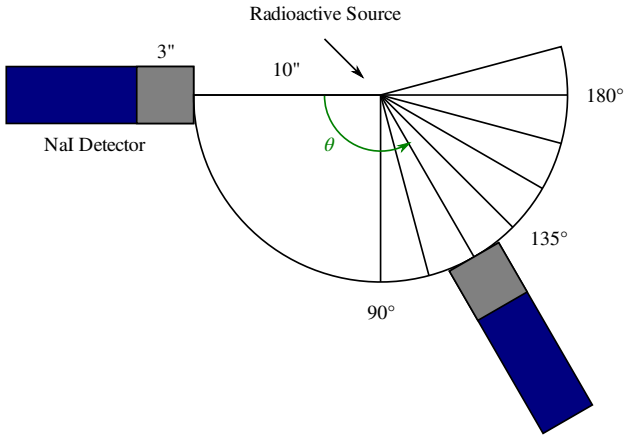

FIG. 3: Schematic of detector array (top-down view). Components are drawn to scale.

II. PROCEDURE

In order to measure the angular correlation of various radioactive sources, we constructed a detector array composed of two NaI scintillation counters doped with thallium. The surface on which the detectors were placed was marked with angles in 5° increments between 90° and 195° with respect to a reference direction facing the first detector. A 10 in arc ensured that the detector faces were always a constant distance from the source, which was placed at the center. We were able to position the second detector at any of the marked angles along the arc to within $\sigma_\theta = 0.45°$ and $\sigma_r = 1$ mm. Figure 3 presents a sketch of this detection apparatus.

Not all photons produced by the radioactive sources represent pairs of emissions from the same nucleus. To limit our analysis to such pairs, we constructed a coincidence circuit

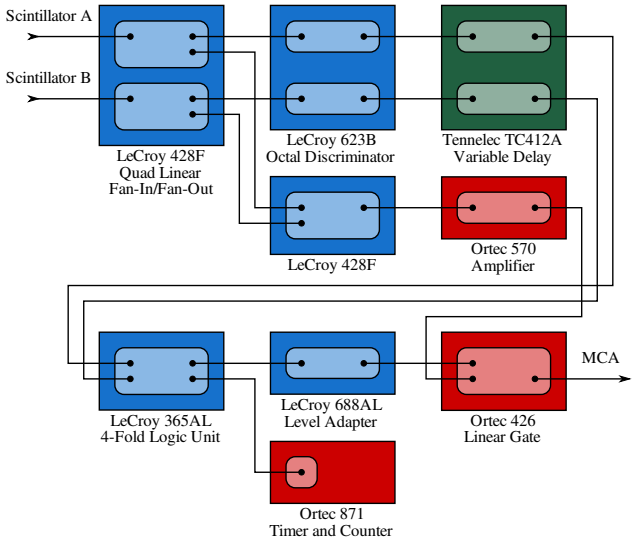

FIG. 4: Schematic of coincidence circuit indicating specific models of relevant NIM modules and their connections.

that would only pass a sum of signals detected simultaneously by both detectors. A discriminator set to its minimum threshold of −30 mV was used to generate logic pulses from detected photons. These were passed through a variable delay and then to a 4-fold logic unit triggering a gate between a linear fan-in and a multichannel analyzer (MCA). In this way, the sums of pulses caused by correlated γ-rays were amplified and delivered to the MCA while extraneous signals were filtered out. We also kept a count of coincidence events to verify the results of the MCA. Figure 4 describes the exact components and connections used in the construction of this circuit.

To account for any relative delays between the two detectors, we measured the coincidence rate of a ^{22}Na source ($\theta = 180°$) for various imposed delays in the two channels. The results are recorded in Table I and plotted in Figure 5, and from them we conclude that a delay of 16 ns in the signal from the first detector is necessary to synchronize the two channels. Furthermore, we see that the resolution of this coincidence circuit, measured as half the full width at half maximum of the plot, is 28 ns. The required imposed delay was verified and monitored throughout the experiment using a fast oscilloscope.

Once the circuit was confirmed to be in-time, we could confidently measure the emission spectra of both the sodium and cobalt sources using the MCA. Placing the gate in "Pulse Inhibit" mode allowed us to measure the non-coincidence spectrum of sodium and thus perform a 2-point calibration of the MCA using its peaks at 511 keV and 1277 keV, as shown in Figure 6. We could further refine this calibration with measurements of the cobalt spectrum, plotted in Figure 7, which clearly show peaks at 1172 keV and 1333 keV.

TABLE I: Measurements of the coincidence rate at various imposed delays between the two detector channels. Positive delays correspond to a delay in the first detector's signal, while negative values indicate a delay for the second detector.

Delay [ns]	Counts per Minute	Delay [ns]	Counts per Minute
-32	402	16	19255
-28	595	20	19534
-24	1079	24	19295
-20	3999	28	19559
-16	12082	32	19276
-12	17621	36	18274
-8	18857	40	13478
-4	18928	44	5371
0	19057	48	1899
4	19222	52	1320
8	19040	56	1209
12	19525	60	1100

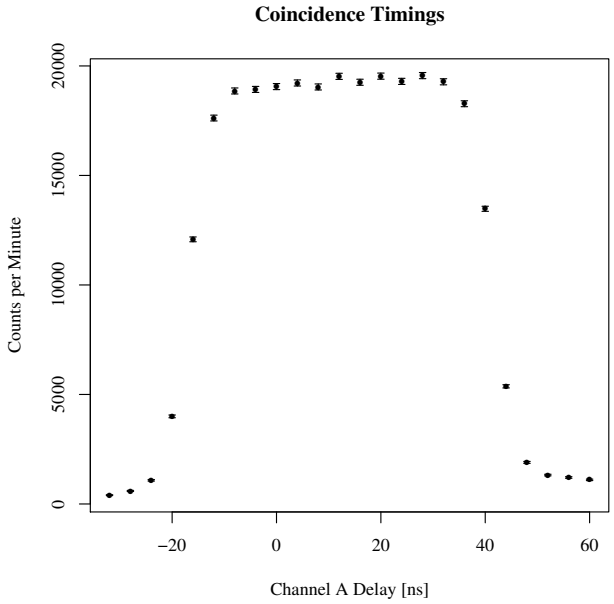

FIG. 5: Plot of coincidence rate versus delay between the two detector channels. The full width at half maximum determines the resolving time of the coincidence circuit.

III. DATA

With the coincidence circuit and MCA properly calibrated, we proceeded to measure the angular correlation of coincidence rates for both ^{22}Na and ^{60}Co. For sodium, we counted the number of events in 1 min starting at $\theta = 180°$ and decrementing θ by 5° until the rate fell to zero. These measurements are tallied in Table II.

For cobalt, we took measurements over 30 min intervals traveling from $\theta = 180°$ to $\theta = 90°$ at 30° increments, then from $\theta = 105°$ to $\theta = 165°$ in order to help compensate for temporal effects. Unfortunately, due to the long integration

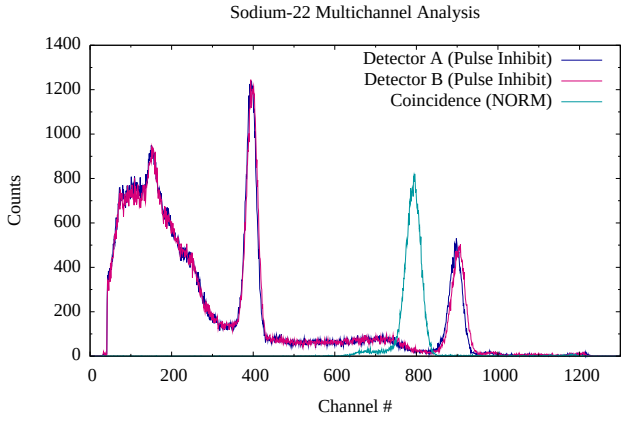

FIG. 6: Emission spectra of sodium-22 for both coincidence and non-coincidence events. Non-coincidence spectra are plotted for both channels to check for equal gain settings.

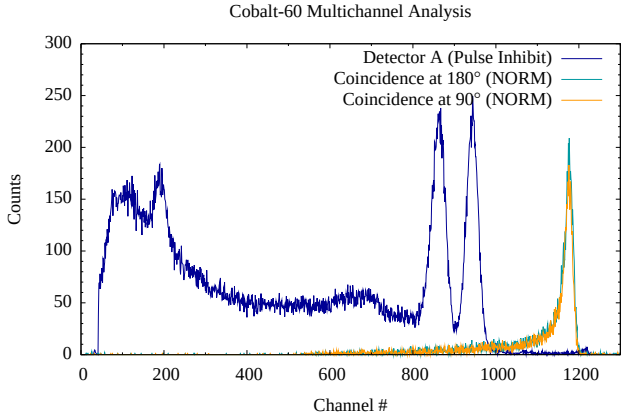

FIG. 7: Emission spectra of cobalt-60 for both coincidence and non-coincidence events.

time required, several of these measurements had to be taken on different occasions. In such cases, a repeat measurement was made at $\theta = 180°$ so that the results could be scaled to match previously-taken data. Both the raw and scaled measurements are recorded in Table III. Due to potential saturation of the linear fan-in unit (indicated by the sharp edge at the right of Figure 7), the coincidence peak in the cobalt spectrum was difficult to define in a consistent manner. Therefore,

TABLE II: Coincidence rates for ^{22}Na in 5° increments. Counts were recorded over 60 s. Net areas (and uncertainties) were computed using the MAESTRO MCA emulator.

θ [°]	Counts	Net Area	$\sigma_{\text{Net Area}}$
180	19460	16450	200
175	12736	10454	168
170	4443	3272	107
165	443	139	31
160	304	0	1

TABLE III: Coincidence rates for ^{60}Co in 15° increments. Counts were recorded over 30 min. Data taken on different occasions are scaled based on overlapping measurements (not shown).

θ [°]	Raw Counts	Corrected Counts	σ_{Counts}
180	8657	—	93
165	8687	8542	171
150	8501	—	92
135	8434	8294	167
120	7695	—	88
105	7329	7611	121
90	7598	—	87

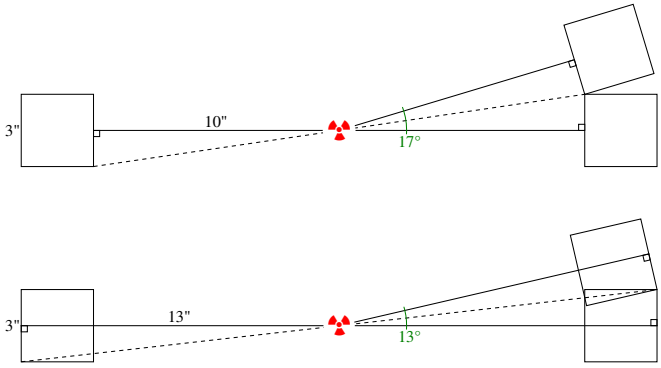

FIG. 8: Analysis in 2 dimensions of the effects of finite detector resolution on the ability to detect γ-rays emitted by pair annihilation. In particular, given the size of our detectors, the coincidence rate should drop to zero around $\theta = 15°$.

we based our analysis on the total count of coincidence events, using Poisson statistics for the error. As the events in the peak clearly dominate the total spectrum, the effects of this choice on the results should be negligible.

IV. RESULTS

Ideally, the angular correlation function for ^{22}Na would be a δ-function centered at $\theta = 180°$ (Equation 1). Due to the finite angular resolution of the detectors, however, this function is smeared over a range of detector angles. A 2-dimensional analysis conducted in the central plane of the detectors, pictured in Figure 8, indicates that the coincidence rate of photons emitted in opposite directions should rapidly approach zero between $\theta = 13°$ and $\theta = 17°$ given the size and separation of our detectors.

Our observations of the angular dependence of coincidence events from sodium, plotted in Figure 9, agree with this analysis. The data is strongly peaked at $\theta = 180°$ and drops to zero between $\theta = 15°$ and $\theta = 20°$.

To further test the extent to which our measurements agree with the theory, we developed a Monte Carlo simulation package able to accommodate custom detector arrays and radioactive sources. Approximating our detectors as circular discs with 100% efficiency, we computed the expected relative coincidence rates for ^{22}Na and plotted them along our data in

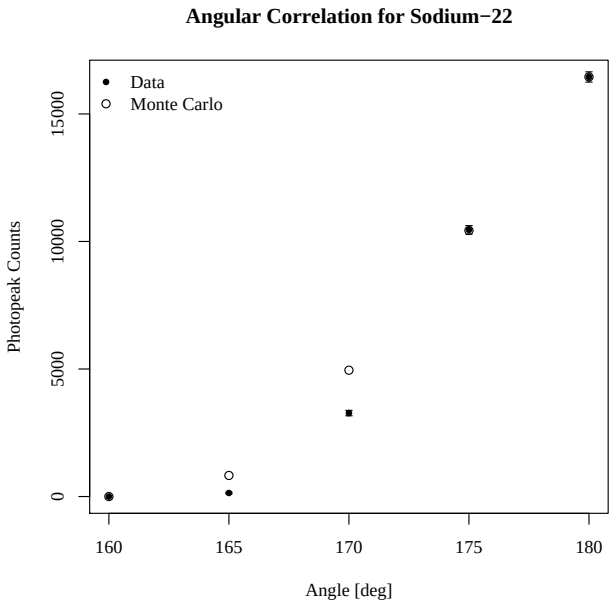

FIG. 9: Measurements and uncertainties of the angular correlation function of sodium-22 based on net photopeak area. Monte Carlo simulation results provide an indication of the effects of finite detector resolution.

Figure 9. The two results agree with each other at the extremes, but diverge for intermediate angles. This is most likely explained by the dependence of the real detectors' efficiency on the incidence angles of the incoming γ-rays. Non-normal γ-rays are less likely to interact with the NaI crystal, which is consistent with the more rapid decrease in coincidence rates compared with the simulation.

As the theoretical angular correlation function for ^{60}60 is finite and smooth, we can fit our measurements to a function of similar form (specifically, a scaled version of Equation 3) and evaluate the agreement of the resulting coefficients with theory. Using the Levenberg-Marquardt method, we find our data to be described by function parametrized by $A_{22} = 0.0977 \pm 0.0099$ and $A_{44} = -0.0011 \pm 0.0125$. The χ^2 for the fit is 5.3, which, on $\nu = 4$ degrees of freedom, implies that deviations from the fit as large as those exhibited by our data set would be expected 26% of the time. Our resulting fit, along with the scaled data, is plotted in Figure 10.

These coefficients are not directly comparable with those of the theoretical correlation function, however. The finite angular acceptance of both detectors smears the correlation function, requiring an adjustment to the theory before the fit can be evaluated for consistency. In the case of cylindrically symmetric detectors, the correction factors can be computed directly via numerical integration if the efficiency of the detectors with respect to the incident angle is known. For these 3 in × 3 in detectors separated from the source by 10 in, the whole-spectrum correction factors are $Q_2 = 0.986$ and $Q_4 = 0.954$, resulting in expected theoretical coefficients of $A_{22} = 0.1020$ and $A_{44} = 0.0091$. These agree with our fit-

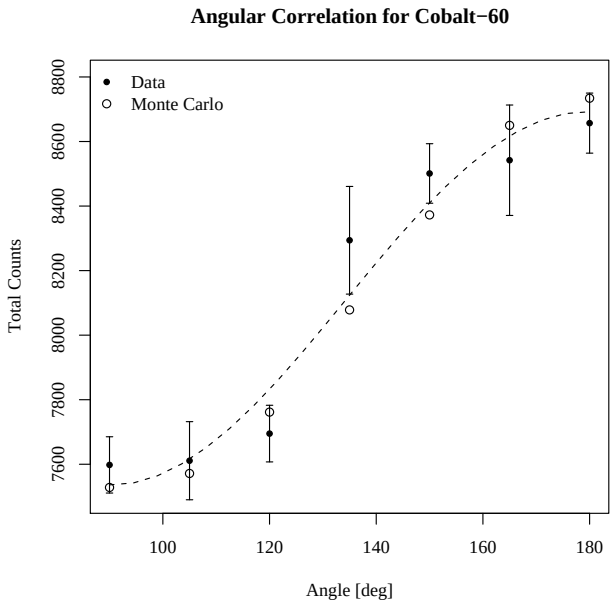

FIG. 10: Measurements and uncertainties of the angular correlation function of cobalt-60 based on total counts. The least squares quadrupole-quadrupole fit is plotted as well. Results from Monte Carlo simulations provide a second means of assessing the effects of finite detector resolution.

ted values given our propagated uncertainties. The precision of our measurements is not great, however, as A_{22} is only determined to within 36%.

As an additional check of the correction factors, we conducted a 2-dimensional Monte Carlo simulation in the central plane of the detectors, which were again represented as 3 in disks with perfect efficiency at all wavelengths and incident angles. We fitted the same form of angular correlation function to the results, plotted in Figure 10, and obtained coefficients statistically consistent with the corrected theoretical coefficients with a χ^2 probability of 19%.

V. CONCLUSION

Our results demonstrate that our theoretical understanding of the angular correlation of γ-rays produced in nuclear decay is accurate to within the uncertainties of our experimental apparatus. In particular, our measurements of sodium-22 are consistent with the δ-function distribution expected from pair annihilation, and our measurements of cobalt-60 agree with those expected from sequential 4-2-0 quadrupole-quadrupole transitions.

While our experimental results were consistent with established theory, uncertainties in our measurements prevent us from extracting strict constraints on that theory. In particular, the long integration times required to minimize statistical uncertainties in the cobalt spectrum forced the data to be gathered on several different occasions, allowing temporal effects in the detection apparatus to accumulate significantly. Additionally, time constraints limited the extent to which we could take overlapping measurements to compensate for these effects. The limited output range of the linear fan-in also deteriorated the quality of our measurements by making analysis of the photopeak impractical.

Future work could improve on our results by providing an environment in which a large number of partially overlapping measurements could be taken in close temporal proximity with a highly stable high voltage power supply. Extending integration times to 45 min or longer would reduce the moderately-sized statistical uncertainties, and scaling uncertainties would be removed entirely. These uncertainties currently dominate the final error and will continue to do so until the separation between data points approaches 1°. The Monte Carlo representation of the cobalt source could also be extended to 3 dimensions to get a better handle on the smearing effects of the detectors' finite angular resolution. Finally, smaller detectors would improve our ability to measure the angular correlation for ^{22}Na.

[1] D. R. Hamilton, Physical Review **58**, 122 (1940).
[2] E. L. Brady and M. Deutsch, Physical Review **78**, 558 (1950).